Available online at www.sciencedirect.com
SCIENCE DIRECT
Journal of Magnetic Resonance 178 (2006) 334–339
JMR Journal of Magnetic Resonance
www.elsevier.com/locate/jmr

Communication

Hadamard frequency-encoded SOFAST-HMQC for ultrafast two-dimensional protein NMR

Paul Schanda, Bernhard Brutscher *

Institut de Biologie Structurale, Jean-Pierre Ebel C.N.R.S.–C.E.A.–UJF 41, rue Jules Horowitz, 38027 Grenoble Cedex, France

Received 1 September 2005; revised 7 October 2005
Available online 2 November 2005

Abstract

We demonstrate the feasibility of recording ^{1}H–^{15}N correlation spectra of proteins in only one second of acquisition time. The experiment combines recently proposed SOFAST-HMQC with Hadamard-type ^{15}N frequency encoding. This allows site-resolved real-time NMR studies of kinetic processes in proteins with an increased time resolution. The sensitivity of the experiment is sufficient to be applicable to a wide range of molecular systems available at millimolar concentration on a high magnetic field spectrometer.

Keywords: Fast NMR; Hadamard spectroscopy; Kinetics; Proteins; Selective pulses

Multidimensional nuclear magnetic resonance (NMR) has proven a useful tool for the structural and dynamical characterization of biological macromolecules. Multidimensional NMR is also very powerful for real-time site-resolved studies of kinetic processes in these biomolecules. An important limitation for such applications, however, remains the intrinsically low time resolution provided by multidimensional NMR because each 2D spectrum requires at least a few minutes, each 3D spectrum a few hours of data acquisition to obtain an acceptable spectral resolution. Recently, there has been an increasing interest in developing new methods for faster multidimensional data acquisition (for a review see [1]). The experimental time required to record a complete spectrum is determined by the number of repetitions of the basic pulse scheme (scan) and the duration of a single scan. The number of repetitions has to take into account phase cycles and quadrature detection, and it determines the spectral resolution in the individual indirect frequency dimensions. The length of a single scan is generally dominated by the time required for the spin system to relax towards its thermal equilibrium after a multiple-pulse sequence (recycle delay). Most approaches proposed for fast NMR data acquisition aim at reducing the number of recorded data points. Examples are projection NMR [2–5], Hadamard NMR [6,7], single scan NMR [8], and non-linear data recording and processing [9–11]. Alternatively, one may reduce the length of a single scan, generally dominated by the time required for the spin system to relax towards its thermal equilibrium after a multiple-pulse sequence (recycle delay). The sensitivity of certain pulse sequences for short recycle delays can be enhanced by the use of spin–lattice relaxation enhancement techniques [12,13] or Ernst-angle excitation [14,15]. Recently we have introduced SOFAST-HMQC [16], an experiment that combines the advantages of spin–lattice relaxation enhancement and Ernst-angle excitation to reduce inter-scan delays. SOFAST-HMQC has proven to provide the required sensitivity to record well-resolved ^{1}H–^{15}N and ^{1}H–^{13}C correlation spectra of proteins at millimolar concentration within a few seconds of acquisition time. IPAP-SOFAST-HMQC, a slightly modified version of the originally proposed experiment, allows application on spectrometers equipped with cryogenic probes [17]. In the IPAP-SOFAST-HMQC experiment the heteronuclear decoupling during acquisition is replaced by an IPAP filter

* Corresponding author. Fax: +33 4 76 88 54 94.
E-mail address: Bernhard.Brutscher@ibs.fr (B. Brutscher).

1090-7807/$ - see front matter © 2005 Elsevier Inc. All rights reserved.
doi:10.1016/j.jmr.2005.10.007

[18,19] thus reducing probe heating and duty cycle problems for the short inter-scan delays required in SOFAST-HMQC. Here, we show that SOFAST-HMQC combined with Hadamard-type frequency editing in the ^{15}N dimension allows to further reduce the minimal experimental time. As demonstrated for the protein ubiquitin this "hybrid" technique, Hadamard-encoded SOFAST-HMQC or IPAP-SOFAST-HMQC, provides site-specific resolution for a large number of nuclei in the protein within one second of data acquisition. This is, to the best of our knowledge, the first time that such 2D spectral information is obtained on a fairly concentrated protein sample (2 mM) in about one second of experimental time using a standard high-field NMR spectrometer. The increased time resolution provided by the Hadamard-encoded SOFAST-HMQC opens the way to real-time investigations of protein kinetics with characteristic time constants of less than a second.

The pulse sequence for Hadamard-encoded SOFAST-HMQC is shown in Fig. 1A. The basic features of Hadamard-encoded SOFAST-HMQC are the same as discussed previously for SOFAST-HMQC [16] except for the ^{15}N time-domain frequency labeling which is replaced by a Hadamard encoding scheme. Therefore only the main features will be summarized shortly. First, ^{1}H pulses are applied band-selectively which ensures that the unobserved protons remain in their equilibrium state and provide a thermal bath of proton spin polarization which enables faster spin–lattice relaxation of the excited ^{1}H spins via dipolar interactions. Second, the first ^{1}H pulse has an adjustable flip angle α that allows further optimization of the sensitivity of the experiment for a chosen (short) scan time. In practice, a flip angle $90° \leqslant \alpha \leqslant 160°$ is chosen to ensure that part of the ^{1}H magnetization is restored along the z-axis by the following 180° pulse. Third, the small number of rf pulses reduces signal loss due to pulse imperfections and B_1 field inhomogeneities, and limits the effects of sample and probe heating. The application of only two (band-selective) ^{1}H pulses also ensures minimal perturbation of the unobserved proton spin polarization, thus optimally exploiting the spin–lattice relaxation enhancement effect discussed above.

In the sequence of Fig. 1A the free evolution delay t_1 of the standard SOFAST-HMQC is replaced by a Hadamard-type ^{15}N frequency encoding. In Hadamard spectroscopy [6] N different frequency "channels" or "bands" are defined (Fig. 1B) and each band is manipulated individually by means of frequency-selective radio-frequency (rf) pulses. One may distinguish between *frequency-selective Hadamard* spectroscopy where the band width covered by the selective encoding pulses equals the line width of the individual resonances in the Hadamard-encoded frequency dimension, or *band-selective Hadamard* spectroscopy, where larger band widths are chosen resulting in the projection of all resonance lines within this band on a single point along the Hadamard dimension. The sign of the NMR signal originating from the N bands is changed according to a

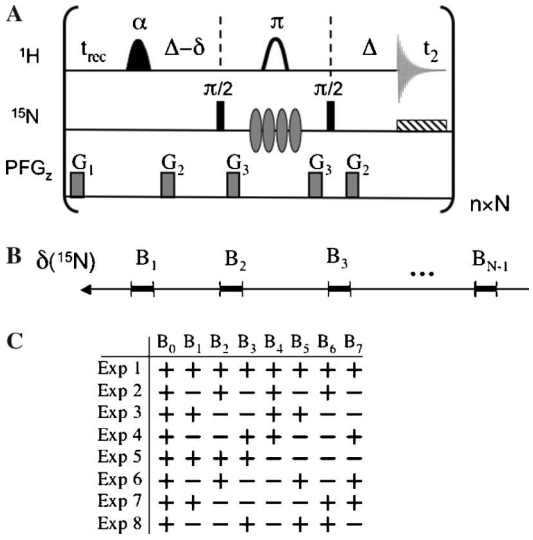

Fig. 1. (A) Hadamard-encoded SOFAST-HMQC pulse sequence to record fast ^{1}H–^{15}N correlation spectra of proteins. The flip angles of the individual rf pulses, all applied along the x-axis, are given above the pulse symbols. Shaped pulse symbols indicate the use of band-selective pulses. The pulse with variable flip angle α has a polychromatic PC9 shape [21] and band-selective ^{1}H refocusing is realized using a REBURP profile [22]. The transfer delay Δ is set to $1/2J_{HN}$, the delay δ accounts for spin evolution during the PC9 pulse, and is adjusted to yield pure phase spectra in the ^{1}H dimension. t_{rec} is the recycle delay between scans. Adiabatic WURST-2 decoupling [23] is applied on X during detection. Hadamard ^{15}N frequency labeling is realized using band-selective refocusing pulses with a sinc profile. The phase of these pulses is interchanged between x and y to realize (+) and (−) encoding, respectively, according to the appropriate Hadamard matrix. The Hadamard encoding pulses were generated by vector addition of the individual band-selective pulse shapes [20]. (B) For Hadamard encoding N different (non-overlapping) frequency bands are defined in the ^{15}N spectrum. N experiments need to be recorded with a sign encoding according to a Hadamard matrix of order N. The same matrix is then used to disentangle the NMR signals from the individual frequency bands during data processing. The Hadamard matrix for the case $N = 8$ is shown in (C). The all-(+) frequency band (B_0) is prone to experimental artifacts and is not used. Therefore, only $N - 1$ frequency bands have to be defined, although N experiments are recorded. If necessary the experiment may be repeated n-times in order to increase the signal-to-noise ratio. The pulse sequence (Varian language) is available from the authors upon request.

Hadamard matrix of order N (Fig. 1C). This sign encoding ensures that each frequency band contributes fully to the detected signal in each of the experimental repetitions, thus providing the same multiplex advantage as standard time-domain NMR spectroscopy. N experiments need to be recorded to separate the individual bands during the processing stage by an inverse Hadamard transformation. The main interest of Hadamard spectroscopy is that the number of bands, and thus the number of repetitions of the experiment, can be freely adjusted without compromising spectral resolution, as long as a Hadamard matrix exists for this particular choice (Hadamard matrices exist for orders $N = 4j$ and $N = 2^j$ with j an integer).

Hadamard frequency encoding in the sequence of Fig. 1A is realized by band-selective ^{15}N refocusing pulses with phase $+x$ for (+) encoding and $+y$ for (−) encoding. The individual band-selective refocusing pulses are

combined to a single shape by vector addition [20], and a different shaped pulse is applied for each of the N experiments. In addition, a ^{1}H 180° pulse is applied simultaneously to the Hadamard encoding pulses to refocus ^{1}H chemical shift evolution. The heteronuclear J_{NH} coupling evolution, however, is not refocused by this 180° pulse sandwich. For NH spin systems the multiple quantum coherence remains unaffected by scalar J_{NH} coupling evolution during the Hadamard encoding. For NH_2 spin systems, however, the peak intensities in the Hadamard-encoded SOFAST-HMQC spectrum are modulated as a function of the encoding time. Proper adjustment of the delay between the two 90° ^{15}N pulses thus allows filtering out signals from NH_2 spin systems. An example of a Hadamard-encoded SOFAST-HMQC experiment is shown in Fig. 2 for the small protein ubiquitin (76 residues). From a standard ^{1}H–^{15}N correlation map a total of seven ^{15}N frequency bands were selected, distributed over the whole frequency range as shown in Fig. 2A. An additional "dummy" band was assigned to the all-(+) frequency band (B_0) that contains signals from ^{15}N spins whose chemical shifts are not or only partially refocused by the Hadamard encoding pulses (see Fig. 3). Our principal aim was to detect as many peaks as possible in the Hadamard-encoded ^{1}H–^{15}N correlation spectrum without too much of peak overlap in the ^{1}H dimension. Therefore, five bands were equally spaced along the ^{15}N dimension ($\Delta\nu = 190$ Hz) in the most crowded spectral region, and two additional bands were defined in the down-field region comprising only little resonances. Different band-selective refocusing pulse shapes were tested to realize band-selective Hadamard encoding of about 3 ppm band width (corresponding to 180 Hz on a 600 MHz spectrometer). Bloch simulations of the spin evolution during the Hadamard ^{15}N encoding using *Gaussian*, sinc or *rSNOB* shapes are shown in Fig. 3. The best compromise between short pulse length and high selectivity was obtained from sinc pulses, truncated after the first side lobe. The result of a Hadamard-encoded ^{1}H–^{15}N SOFAST-HMQC experiment performed with sinc-encoding pulses (pulse length of 22 ms at 60 MHz ^{15}N frequency) and $N = 8$ is shown in Fig. 2B. The spectrum was recorded on a 2 mM sample of ubiquitin (25 °C, pH 6.2) on a 600 MHz Varian INOVA spectrometer equipped with a standard (non cryogenic) triple-resonance probe. The series of 1D spectra corresponds to projections of the 2D spectrum (Fig. 2A) along the ^{15}N dimension over the individual bands. No signals from the NH_2 groups in Asn and Gln side chains are detected in this spectrum, because they are filtered out by the J_{NH} coupling evolution during the chosen Hadamard encoding pulse length. Repeating the whole experiment 64 times (n) increased the signal-to-noise ratio, and allowed to evaluate the spectral quality and to detect artifacts induced by this particular Hadamard encoding. As can be appreciated from Fig. 2B the individual spectra show little artifacts, and correspond to quite nicely resolved 1D amide proton spectra of ubiquitin. Once the feasibility of our method demonstrated, we have repeated the same experiment in only about 1 s of acquisition time by setting $n = 1$. The resulting spectrum is shown in Fig. 4. Despite the reduced

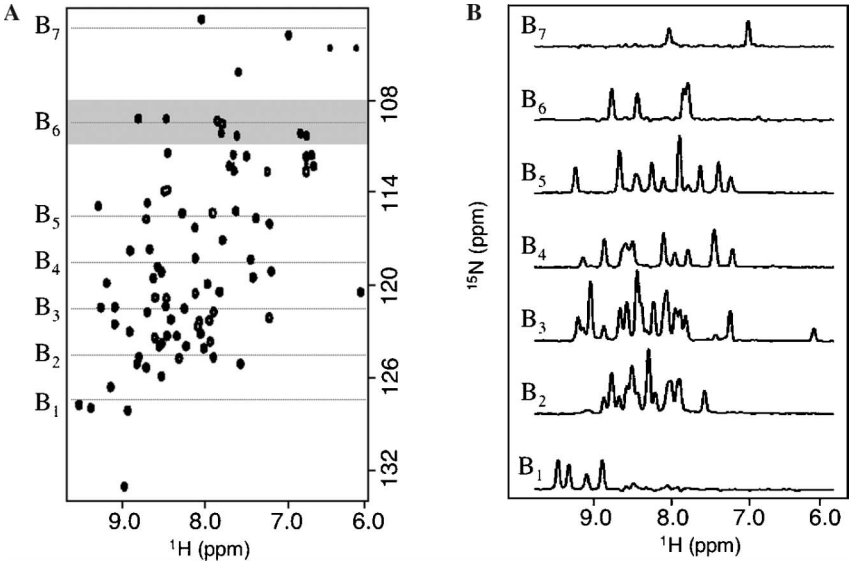

Fig. 2. (A) Definition of the ^{15}N frequency bands used for the Hadamard-encoded SOFAST-HMQC spectrum of ubiquitin shown in (B). The center positions of the individual ^{15}N frequency bands are indicated by dotted lines. The band width of about 3 ppm covered by the Hadamard encoding pulses used for recording spectrum (B) is exemplified for band B_6. The spectrum in (A) has been recorded with a standard ^{1}H–^{15}N HSQC-sequence as provided by the Varian BioPack. The spectrum in (B) has been recorded on a 600 MHz spectrometer on a 2mM sample of ubiquitin (pH 6.2, 25 °C) using the pulse sequence of Fig. 1A with the following parameter settings: $\alpha = 130°$, $\Delta = 5.4$ ms, $\delta = 1.6$ ms, $t_{rec} = 10$ ms, $t_2^{max} = 40$ ms, $N = 8$, $n = 64$ (+4 dummy scans). The band-selective ^{1}H excitation (PC9) and refocusing pulses (REBURP) were centered at 8.0 ppm covering a bandwidth of 4.0 ppm, resulting in pulse lengths of 3.0 ms (PC9) and 2.03 ms (REBURP). The Hadamard encoding pulses were applied with a sinc shape truncated after the first side lobe and a pulse length of 22 ms covering an effective band width of about 180 Hz (3 ppm). ^{15}N decoupling during t_2 was realized using WURST-2 [23] at an average field strength of $\gamma B_1/2\pi = 550$ Hz. The experimental time was 1 min.

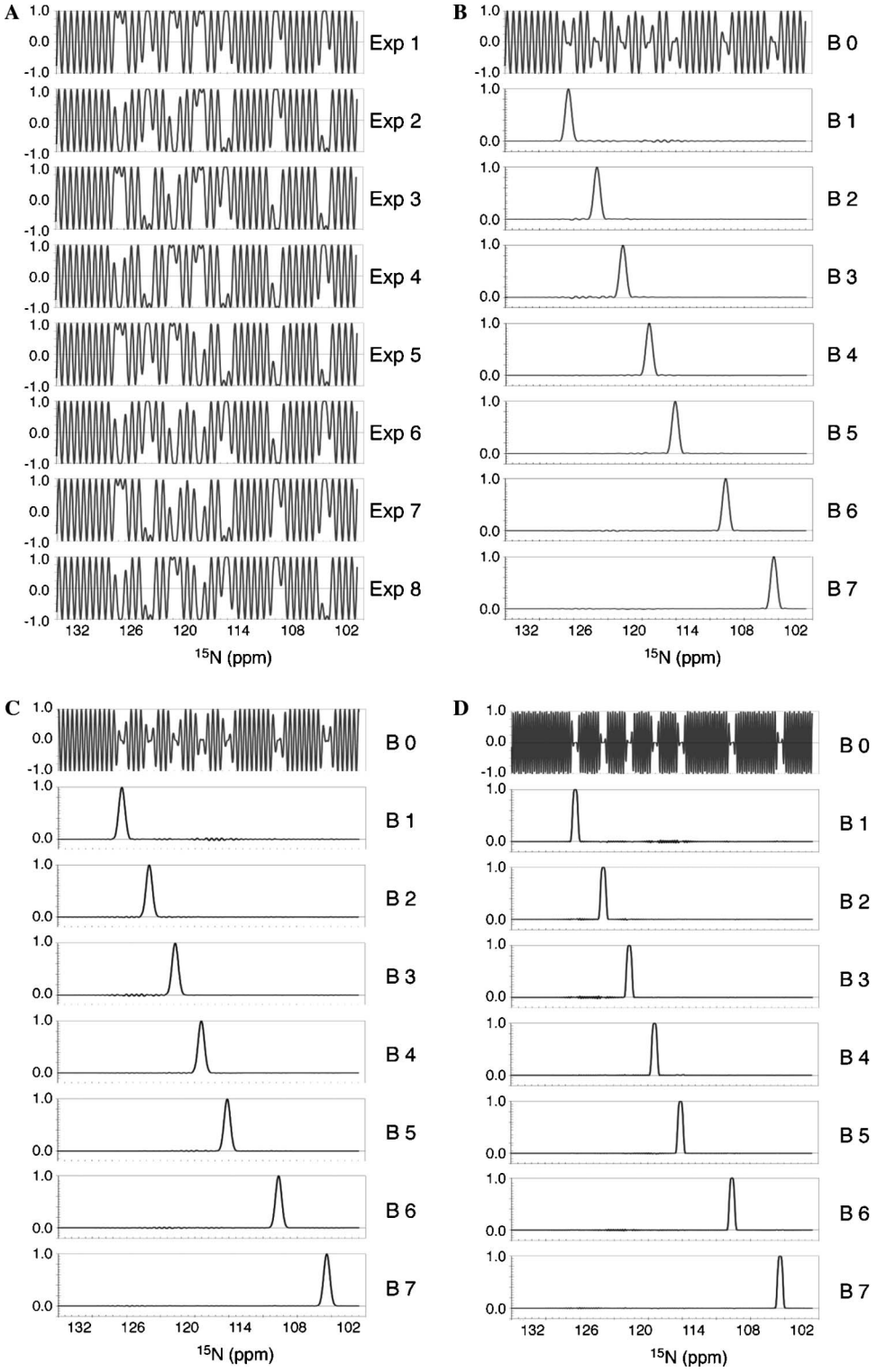

Fig. 3. Bloch simulations of the spin evolution during Hadamard ^{15}N encoding based on the frequency bands defined in Fig. 2A. The calculations, performed using the Varian "Pulsetool," assume an initial N_y state of the spin system and neglect spin relaxation effects. The N_y component present after the Hadamard encoding pulses is plotted. (A) Refocusing performance of the Hadamard pulses used for the different experiments (Exp. 1–Exp. 8) as a function of the ^{15}N frequency for a *sinc* shape (1 side lobe) of 22 ms length. (B) Same simulations as in (A), but the plots correspond to the results after decoding with the appropriate Hadamard matrix to separate the signals from the individual bands (B_0–B_7). (C) Results obtained for a Gaussian pulse shape (truncation level 0.01) of 30 ms length. (D) Results obtained for a *rSNOB* pulse shape [24] of 62 ms length.

signal-to-noise ratio, because of the short overall experimental time, most of the amide protons in ubiquitin are visible in this spectrum, and a significant number of them is spectrally resolved. Overall we count from the spectrum in Fig. 4, a total of 42 resolved peaks, 11 peaks corresponding to two overlapping resonances, and an additional peak

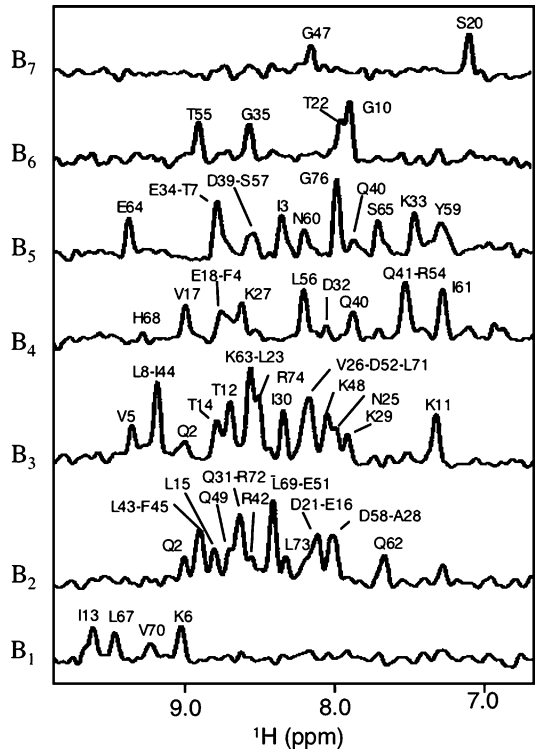

Fig. 4. Ultrafast Hadamard-encoded SOFAST-HMQC spectrum of ubiquitin recorded with the pulse sequence of Fig. 1A. The same frequency bands and acquisition parameters were used as described in Fig. 2, except for the number of repetitions which was set to $N = 8$, $n = 1$ (+4 dummy scans) resulting in an experimental time of about 1 s. Assignments (residue number and type) are shown for the detected amide correlation peaks. 67 amide resonances are detected in this spectrum, out of the 70 cross peaks observed in the standard HSQC spectrum shown in Fig. 2A.

where three resonances superpose. This clearly demonstrates the potential of Hadamard-encoded SOFAST-HMQC for obtaining residue-specific information on a large number of amide sites within one second of experimental time.

In summary, we have shown that site-resolved spectral information can be obtained within one second of acquisition time on a ^{15}N-labeled sample of a small protein at millimolar concentration using a high field NMR spectrometer and Hadamard-encoded SOFAST-HMQC. The experiment can be designed to focus on only a few sites of particular interest using frequency-selective Hadamard encoding, or cover most of the spectral range, as demonstrated here, using band-selective Hadamard encoding. The use of higher field magnets will allow increasing the selectivity of the Hadamard encoding without increasing the lengths of the encoding pulses. It is also possible to adjust the width for each band individually to optimize the number of resolved amide peaks. Higher selectivity will be important for application to larger proteins in order to resolve individual amide sites in the Hadamard-encoded spectra. The reduced sensitivity, because of relaxation losses during the longer Hadamard encoding pulses, may be compensated by the use of cryogenic probes and Hadamard-encoded IPAP-SOFAST-HMQC. The experiment is equally well suited for fast recording of ^{1}H–^{13}C correlation spectra of proteins. Hadamard-encoded SOFAST-HMQC provides a new tool for following the changes in peak intensities occurring during some kinetic event with a seconds resolution for a selected number of nuclear sites. Interesting examples are the measurement of H/D exchange rates, or the measurement of some slow binding kinetics. It is less suited for monitoring processes that do not only change the peak intensities but also their positions, as frequency changes in the ^{15}N dimension within one band do not translate into changes in the Hadamard-encoded spectra. Hadamard-encoded SOFAST-HMQC is only one example of what one could call "hybrid" fast acquisition methods. It is equally possible to combine SOFAST-HMQC with spatial frequency encoding ("single-scan" NMR) or the use of non-linear data acquisition and processing schemes. If the intrinsic sensitivity of NMR spectrometers continues to increase as observed over the last decade, one may expect that such (ultra-) fast acquisition schemes will soon become applicable to a wide range of biomolecular systems.

Acknowledgments

This work was supported by the Commissariat à l'Energie Atomique and the Centre National de la Recherche Scientifique. P.S. acknowledges support from the French ministry of education, research, and technology, and from the Austrian federal ministry of education, science, and culture. The authors thank Isabel Ayala for the preparation of the ^{15}N-labeled ubiquitin sample.

References

[1] R. Freeman, E. Kupce, New methods for fast multidimensional NMR, J. Biomol. NMR 27 (2003) 101–113.
[2] T. Szyperski, G. Wider, J.H. Bushweller, K. Wuthrich, Reduced dimensionality in triple-resonance NMR experiments, J. Am. Chem. Soc. 115 (1993) 9307–9308.
[3] B. Brutscher, J.P. Simorre, M.S. Caffrey, D. Marion, Design of a complete set of 2-dimensional triple-resonance experiments for assigning labeled proteins, J. Magn. Reson. B 105 (1994) 77–82.
[4] S. Kim, T. Szyperski, GFT NMR, a new approach to rapidly obtain precise high-dimensional NMR spectral information, J. Am. Chem. Soc. 125 (2003) 1385–1393.
[5] E. Kupce, R. Freeman, Projection-reconstruction technique for speeding up multidimensional NMR spectroscopy, J. Am. Chem. Soc. 126 (2004) 6429–6440.
[6] E. Kupce, T. Nishida, R. Freeman, Hadamard NMR spectroscopy, Prog. Nucl. Magn. Reson. Spectrosc. 42 (2003) 95–122.
[7] B. Brutscher, Combined frequency- and time-domain NMR spectroscopy. Application to fast protein resonance assignment, J. Biomol. NMR 29 (2004) 57–64.
[8] L. Frydman, T. Scherf, A. Lupulescu, The acquisition of multidimensional NMR spectra within a single scan, Proc. Natl. Acad. Sci. USA 99 (2002) 15858–15862.
[9] V.A. Mandelshtam, The multidimensional filter diagonalization method-I. Theory and numerical implementation, J. Magn. Reson. 144 (2000) 343–356.
[10] J.C. Hoch, A.S. Stern, Maximum entropy reconstruction, spectrum analysis and deconvolution in multidimensional nuclear magnetic resonance, NMR Biol. Macromol. Pt. A (2001) 159–178.

[11] D. Rovnyak, D.P. Frueh, M. Sastry, Z.Y.J. Sun, A.S. Stern, J.C. Hoch, G. Wagner, Accelerated acquisition of high resolution triple-resonance spectra using non-uniform sampling and maximum entropy reconstruction, J. Magn. Reson. 170 (2004) 15–21.
[12] K. Pervushin, B. Vogeli, A. Eletsky, Longitudinal H-1 relaxation optimization in TROSY NMR spectroscopy, J. Am. Chem. Soc. 124 (2002) 12898–12902.
[13] H.S. Atreya, T. Szyperski, G-matrix Fourier transform NMR spectroscopy for complete protein resonance assignment, Proc. Natl. Acad. Sci. USA 101 (2004) 9642–9647.
[14] R. Ernst, G. Bodenhausen, G. Wokaun, Principles of Nuclear Magnetic Resonance in One and Two Dimensions, Oxford University Press, Oxford, 1987.
[15] A. Ross, M. Salzmann, H. Senn, Fast-HMQC using Ernst angle pulses: an efficient tool for screening of ligand binding to target proteins, J. Biomol. NMR 10 (1997) 389–396.
[16] P. Schanda, B. Brutscher, Very fast two-dimensional NMR spectroscopy for real-time investigation of dynamic events in proteins on the time scale of seconds, J. Am. Chem. Soc. 127 (2005) 8014–8015.
[17] P. Schanda, E. Kupce, B. Brutscher, SOFAST-HMQC experiments for recording two-dimensional heteronuclear correlation spectra of proteins within a few seconds, J. Biomol. NMR (2005) in press.
[18] P. Andersson, J. Weigelt, G. Otting, Spin-state selection filters for the measurement of heteronuclear one-bond coupling constants, J. Biomol. NMR 12 (1998) 435–441.
[19] M. Ottiger, F. Delaglio, A. Bax, Measurement of J and dipolar couplings from simplified two-dimensional NMR spectra, J. Magn. Reson. 131 (1998) 373–378.
[20] E. Kupce, R. Freeman, Techniques for multisite excitation, J. Magn. Reson. 105A (1993) 234–238.
[21] E. Kupce, R. Freeman, Wide-band excitation with polychromatic pulses, J. Magn. Reson. A 108 (1994) 268–273.
[22] H. Geen, R. Freeman, Band-selective radiofrequency pulses, J. Magn. Reson. 93 (1991) 93–141.
[23] E. Kupce, R. Freeman, Optimized adiabatic pulses for wideband spin inversion, J. Magn. Reson. A 118 (1996) 299–303.
[24] E. Kupce, J. Boyd, I.D. Campbell, Short selective pulses for biochemical applications, J. Magn. Reson. B 106 (1995) 300–303.